

Dynamic Analysis of Rotor-Ball Bearing System of Air Conditioning Motor of Electric Vehicle

Van-Trang Nguyen¹, Pyung Hwang²

¹Faculty of Vehicle and Energy Engineering, Ho Chi Minh City University of Technology and Education, Ho Chi Minh city, Vietnam

²School of Mechanical Engineering, Yeungnam University, North Gyeongsang, Korea

Email address:

trangnv@hcmute.edu.vn (Van-Trang N.)

To cite this article:

Van-Trang Nguyen, Pyung Hwang. Dynamic Analysis of Rotor-Ball Bearing System of Air Conditioning Motor of Electric Vehicle.

International Journal of Mechanical Engineering and Applications. Special Issue: Transportation Engineering Technology — part II.

Vol. 3, No. 3-1, 2015, pp. 22-28. doi: 10.11648/j.ijmea.s.2015030301.14

Abstract: Nowadays, electric vehicles (EV) present a promising solution to reduce greenhouse gas emissions. They are considered zero emission vehicles. Rotor bearing system is important part of air conditioning motor of EV. The aim of this research is to develop a numerical model to investigate the structural dynamic response of the rigid rotor supported on deep groove ball bearings. The numerical model considers rotor imbalance that varies with speed, as well as sources of nonlinearity such as Hertzian contact force, ball clearance and varying compliance vibration. This is very important on the design point of view. The 4th order Runge-Kutta numerical integration technique has been applied. The results are presented in form of time displacement response, frequency spectra, and Poincaré map. The analysis demonstrates that the number of balls is one of the key factors affecting on the dynamic characteristics of rotor bearing system. The model can also be used as a tool for predicting nonlinear dynamic behavior of rotor system of air conditioning motor of electric vehicle under different operating conditions. Moreover, the study may contribute to a further understanding of the nonlinear dynamics of rotor bearing system.

Keywords: Ball Bearing, Nonlinear Dynamic Response, Chaotic Vibration, Poincaré Map, Varying Compliance Frequency

1. Introduction

Dynamic analysis has been an important field in many engineering applications such as turbines, jet engines, compressor, and electric motor. The prediction and analysis of the dynamic behavior of rotor systems is important because their rotating components possess amounts of energy that can transform into vibrations. These vibrations not only reduce the performance of motor, but may also cause serious damage to the rotating machinery and the entire system. Hence this field has become more challenging since nonlinear analysis is far more difficult compared to the analysis of the linear phenomena. Nonlinearities in rotor systems can occur as a result of many reasons [1] such as Hertzian contact force, internal radial clearance, surface waviness [2], stiffness coefficient.

During the past decades, the literature related to a rotor supported on oil sliding bearing phenomena is abundant. However, the dynamic model of a rotor supported on ball bearing is still very immature [2]. Dong-Soo Lee and Dong Hoon Choi [3] used transfer matrix method to obtain nonlinear dynamic behavior of rotor ball bearing system. El-Saeidy [4]

developed rotating shaft finite element model to predict the dynamic behavior of rotor shaft rolling bearing system with bearing nonlinearities. Tiwari [5, 6] showed experimentally that bearing clearance changes the response of rotor significantly because of the changes in dynamic stiffness of the bearing. Wardle and Poon [7] pointed out the relations between the number of balls and waves for severe vibrations. Wardle showed that ball waviness produced vibrations in the axial and radial directions at different frequencies and also pointed out that only even order of ball waviness produced vibrations [8].

Clearance is provided in the design of bearing to compensate for the possible thermal expansion; it is also the source of vibration and introduces nonlinearity in the dynamic behavior. From literature, there is not much work done on the nonlinear dynamic response of unbalanced rigid rotor mounted on deep groove ball bearing with radial internal clearance and the number of balls, which have been attempted in present work.

The aim of this work is to develop a numerical model for investigating the influence of number of balls on the dynamic

characteristic of rigid rotor supported on ball bearing. A two-degree of freedom system is considered with the assumption that there is no friction between the rolling elements and raceways of ball bearings. The rolling elements are positioned symmetrically such that their motion is in synchronized. The 4th order Runge-Kutta numerical integration technique has been used to solve the system of nonlinear differential equations iteratively. The results present here have been obtained from huge number of numerical integrations; and are mainly in form of time displacement response, frequency spectra, and Poincaré maps. The analysis demonstrates that the number of balls is one of the key factors affecting on the dynamic characteristics of rotor bearing system [16]. The results provide a reliable model for predicting dynamic behavior of rotor ball bearing system under different operating conditions. This is of the utmost importance in the design stages of rotating machinery systems.

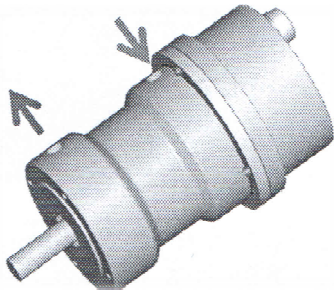


Figure 1. A typical air conditioning motor system of EV.

2. Problem Formulation

Since a real rotor bearing system is extremely complex and difficult to model, the analysis of the dynamic behavior of the system can still be obtained based on the following assumptions while developing the mathematical model:

1. Torsional vibration of rotor and gyroscopic effects may be neglected and only transverse vibration of rotor should be considered.
2. The outer race of the ball bearing is fixed to a rigid support and the inner race is fixed rigidly to the shaft and there is no slipping of balls.
3. Constant vertical radial force acts on the bearing.
4. Elastic deformation between race and ball gives a nonlinear force deformation relation, which is obtained by using Hertzian theory.

Zeillinger and K Kötritsch [9] noted that additional damping usually occurs between the bearing outer race and its housing. It is known that ball bearing have very low inherent damping. That is due to friction and small lubrication. However little information is available on actual damping coefficients. This damping would be effective only for small vibration amplitude [10]. Krämer [11] has provided as estimation of the bearing damping and [12] also the bearing coefficient of ball bearing is well within the range of 33.75 Ns/m to 337.5 Ns/m. A value of $c = 200$ Ns/m was chosen. The rotor-bearing system is modeled with two degrees of freedom and the bearings are

modeled to be nonlinear; it is shown schematically in Fig. 2.

Table 1. Geometrical properties of the system.

Inner race radius, R_b (mm)	9.37
Outer race radius, R_a (mm)	14.43
Ball diameter, D (mm)	4.762
Radial clearance, γ (μm)	2
Radial load, W (N)	6
Mass of rotor, m (kg)	1.2
Rotor speed (rpm)	5,500
Damping factor, c (Ns/m)	200
Number of the ball, N	11
Time step, Δt (s)	10^{-5}
Elastic modulus, E (N/mm ²)	2.08×10^5
Poisson's ratio	0.3

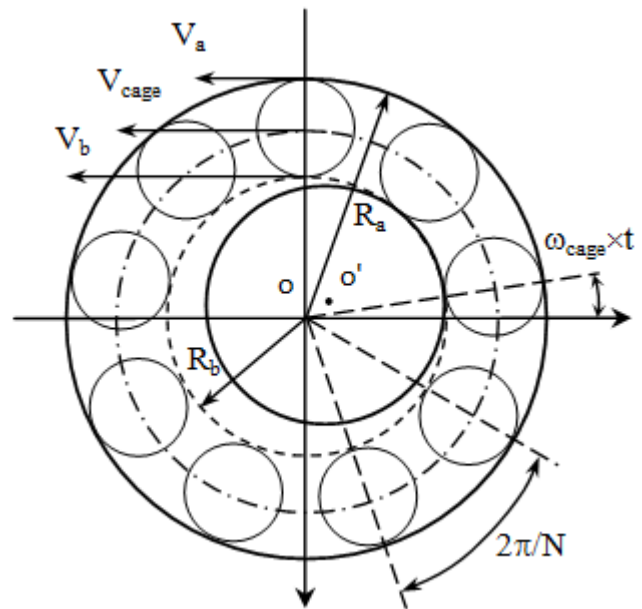


Figure 2. Schematic diagram of a typical ball bearing.

2.1. Nonlinear Ball Bearing Force

As shown in Fig. 2, the tangent velocity of the contact point between the ball and the inner race V_a , outer race V_b , respectively, can be given by

$$V_a = 0 \quad (1)$$

$$V_b = \omega_b \cdot R_b \quad (2)$$

Since the outer race is assumed to be stationary, $V_a = 0$. Therefore, the tangent velocity of the cage is

$$V_{cage} = \frac{1}{2}(V_a + V_b) = \frac{V_b}{2} = \frac{\omega_b \times R_b}{2} \quad (3)$$

Because the inner race is fixed to the shaft, $\omega_b = \omega_{rotor}$. Then, the angular velocity of the cage is written by

$$\omega_{cage} = \frac{V_{cage}}{(R_a + R_b)/2} = \omega_{rotor} \times \frac{R_b}{R_a + R_b} \quad (4)$$

The varying compliance frequency or the ball passage frequency can be expressed in terms of the cage speed times the number of balls, N .

$$\omega_{vc} = \omega_{cage} \times N = \omega_{rotor} \times \left(\frac{R_b}{R_a + R_b} \times N \right) \quad (5)$$

According to the Hertzian contact theory, the local Hertzian contact force F_j between the j^{th} ball and the race is given by [13]

$$F_j = K \times \delta_j^{1.5} \quad (6)$$

The contact stiffness coefficient K , can be given by the stiffness coefficient between the ball and each race [13], k_i and k_0 in series as follows:

$$K = \frac{1}{\left[\left(\frac{1}{k_i} \right)^{\frac{2}{3}} + \left(\frac{1}{k_0} \right)^{\frac{2}{3}} \right]^{\frac{3}{2}}}, \quad (7)$$

where k_i and k_0 can be determined by elastic modulus and Poisson's ratio and curvature sum of the contact points as from Harris [13]. A deep groove ball bearing (NSK 6002) which is widely used in electric motors. The main bearing parameters are listed in Table 1; and $K = 7.055 \times 10^9$ (N/mm^{1.5}).

The inner race is supported by the rolling balls over an angular contact zone. Base on the Hertzian contact force between inner and outer race and the ball, the total restoring force is the sum of restoring force from each of the rolling elements. The "+" sign as a subscript in the equation (8,9) signifies that the expression within the brackets must be greater than zero. If the expression inside the brackets is negative, then the rolling element is not in the load zone, and restoring force is set to zero [15]. If the expression within the brackets is greater than zero, then the ball at the angular location θ_j is within the angular contact zone and it is loaded giving rise to a restoring force. Hence the contact force between the j^{th} ball and inner race can be expressed as

$$F_x = \sum_{j=1}^N K \left[(x \cos \theta_j + y \sin \theta_j) - \gamma \right]_+^{1.5} \cos \theta_j \quad (8)$$

$$F_y = \sum_{j=1}^N K \left[(x \cos \theta_j + y \sin \theta_j) - \gamma \right]_+^{1.5} \sin \theta_j \quad (9)$$

As shown in Fig. 2, the inner race is moving at the speed of the shaft and the ball center at the speed of the cage so the angular location of j^{th} ball θ_j can be obtained from

$$\theta_j = \frac{2\pi}{N} (j-1) + \omega_{cage} \times t; \quad j = 1, \dots, N \quad (10)$$

2.2. Equations of Motion

The mathematical model takes into account the sources of nonlinearities in rotor bearing system. After assembling the inertia, ball bearing force, damping force, and constant vertical force acting on the inner race, the dynamic equations of the system is two coupled nonlinear ordinary second order differential equations having parametric effect, the 1.5 nonlinearity and the summation term as (11a) and (11b):

$$m\ddot{x} + c\dot{x} + \sum_{j=1}^N K \left[(x \cos \theta_j + y \sin \theta_j) - (\gamma) \right]_+^{1.5} \cos \theta_j = W + F_u \cos(\omega_{rotor} t) \quad (11a)$$

$$m\ddot{y} + c\dot{y} + \sum_{j=1}^N K \left[(x \cos \theta_j + y \sin \theta_j) - (\gamma) \right]_+^{1.5} \sin \theta_j = F_u \sin(\omega_{rotor} t) \quad (11b)$$

3. Results and Discussion

The system equations of motion (11) are nonlinear second order differential equations. They are solved by the 4th order Runge-Kutta method to obtain the axial and radial displacement of the shaft. The time step for the direct numerical integration is 10⁻⁵ (s). The initial displacement are set: $x_0 = y_0 = 10^{-6}$ (m); the initial velocities are set to be zero: $\dot{x}_0 = \dot{y}_0 = 0$ (m/s). The inner race rotates at a constant speed of 5,500 rpm.

Table 2. Classification of Poincaré maps

Poincaré map	Motion state
Single point	Synchronous
n discrete points	nT-Periodic
Closed curve formed by infinite points	Quasi-periodic
Dense points	Chaotic

Poincaré sections are the stroboscopic picture of the motion in a phase plane that will be obtained by plotting the vertical or horizontal displacement against its derivative, once per rotational period T ($T = 2\pi/\omega$) of the system. The projection of Poincaré section on the $x(nT)$ - $y(nT)$ plane is referred to as Poincaré map of the motion. It is also indicated the nature of the motion. According to Francis C. Moon [14], characteristics of different typical motion states in the Poincaré maps are shown in Table 2. In order to observe the effect of the number of balls, time displacement response, Poincaré maps, and frequency domain vibration of rotor bearing system are obtained to determine the dynamic behavior of system. The number of the balls are set to 9, 10, 11, respectively.

The number of balls is one of the key factors affecting on the dynamic characteristics of a rotor system. Fig. 3 shows the response with 9 balls. The natural frequency coincides with the varying compliance frequency ($\omega_{vc} = 324$ Hz). The peak amplitude is 0.08 μm on horizontal direction. For horizontal displacement response, the major peaks amplitude of vibration appear at $8\omega_{vc}/5 = 520$ Hz, $2\omega_{vc} = 650$ Hz, and

$13\omega_{vc}/5 = 844$ Hz. The amplitude of peak is $0.287 \mu\text{m}$ on vertical direction at $\omega_{vc} = 324$ Hz. The other major peaks for vertical displacement response are at $8\omega_{vc}/5 = 520$ Hz, and $2\omega_{vc} = 650$ Hz. The orbits of a fairly dense structure in the Poincaré maps, which give an indication of a chaotic response, as shown in Fig. 3(b), 3(e).

As the number of balls increases, the system stability returns and shows periodic nature and lower peak amplitude of vibration for 10 balls as shown in Fig. 4. The Poincaré maps showed in Fig. 4(b) and 4(e), give an indication of a periodic response because of closed orbit formed by infinite points.

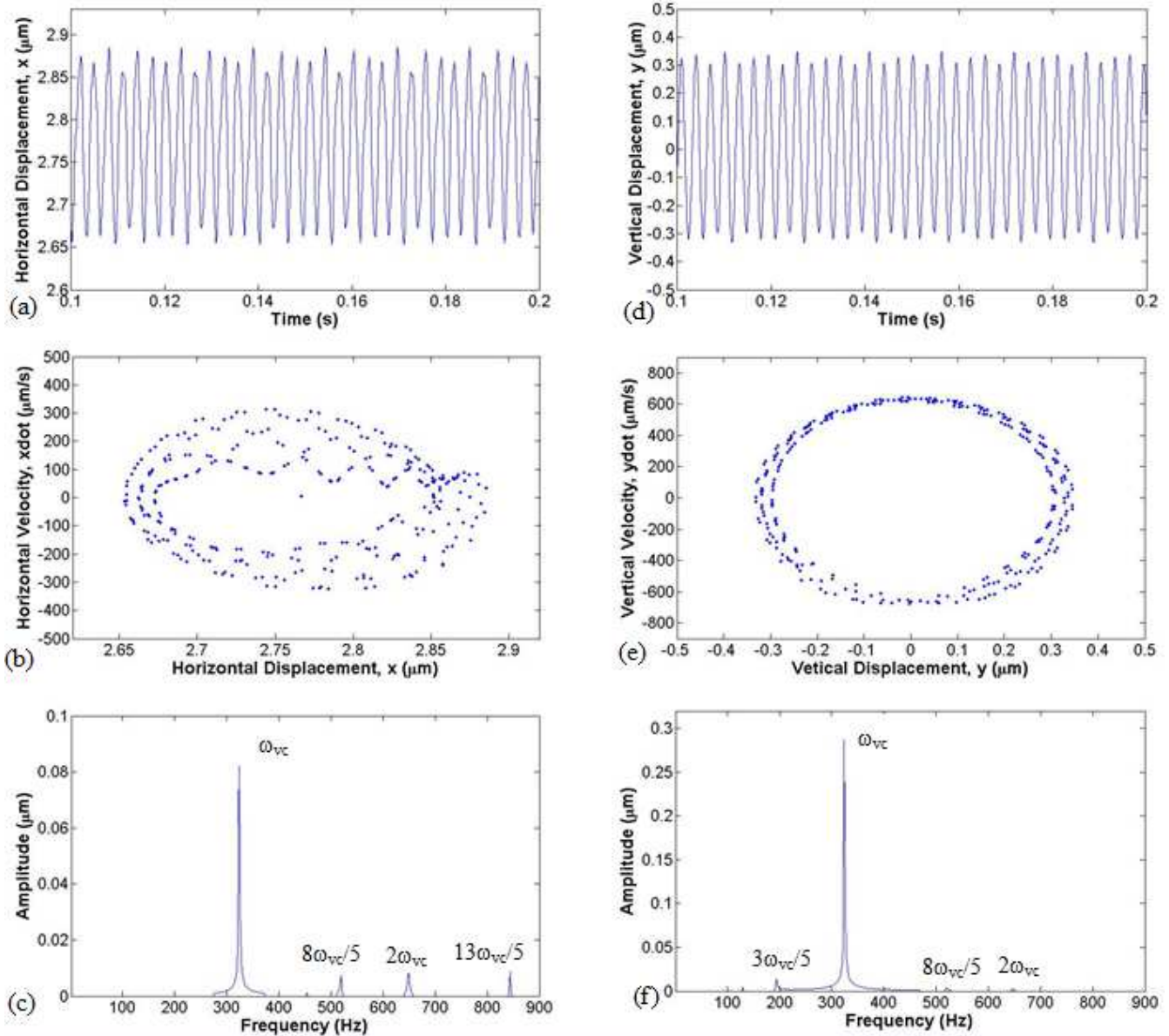


Figure 3. (a), (b), (c) Horizontal displacement response with time, Poincaré map for horizontal displacement response and FFT for horizontal displacement response at $N = 9$, respectively. (d), (e), (f) Vertical displacement response with time, Poincaré map for vertical displacement response, and FFT for vertical displacement response at $N = 9$, respectively.

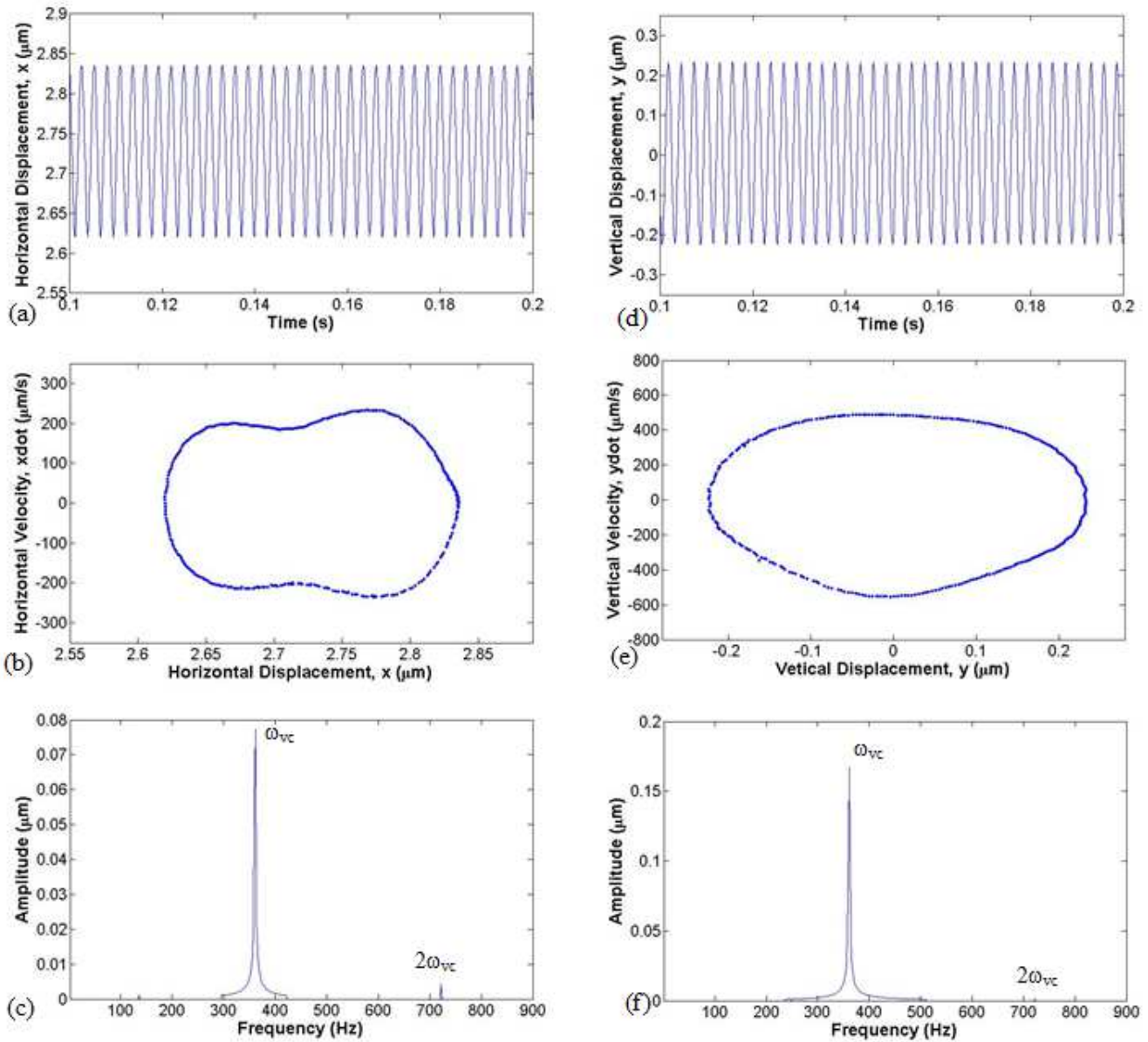


Figure 4. (a), (b), (c) Horizontal displacement response with time, Poincaré map for horizontal displacement response, and FFT for horizontal displacement response at $N = 10$, respectively. (d), (e), (f) Vertical displacement response with time, Poincaré map for vertical displacement response, and FFT for vertical displacement response at $N = 10$, respectively.

The amplitude of peaks for horizontal and vertical displacement response are at 0.077 and $0.167 \mu\text{m}$, respectively. The other major peak for horizontal displacement response is at $2\omega_{vc} = 722 \text{ Hz}$. The other major peak for vertical displacement response is also at $2\omega_{vc} = 722 \text{ Hz}$. Sub-harmonic seem to be disappearing as shown in Fig. 4(c) and 4(f). Hence, the nonlinear dynamic responses are found to be associated with the varying compliance frequency. For the response with 11

balls, the natural frequency coincides with varying compliance frequency ($\omega_{vc} = 396 \text{ Hz}$). The amplitude of peaks for horizontal and vertical displacement response are 0.075 and $0.117 \mu\text{m}$, respectively, as shown in Fig. 5. The Poincaré maps showed in Fig. 5(b) and 5(e), give an indication of a quasi-periodic response because of “net” structure. The other major peaks for horizontal and vertical displacement response are at $2\omega_{vc} = 794 \text{ Hz}$ as shown in Fig. 5(c) and 5(f).

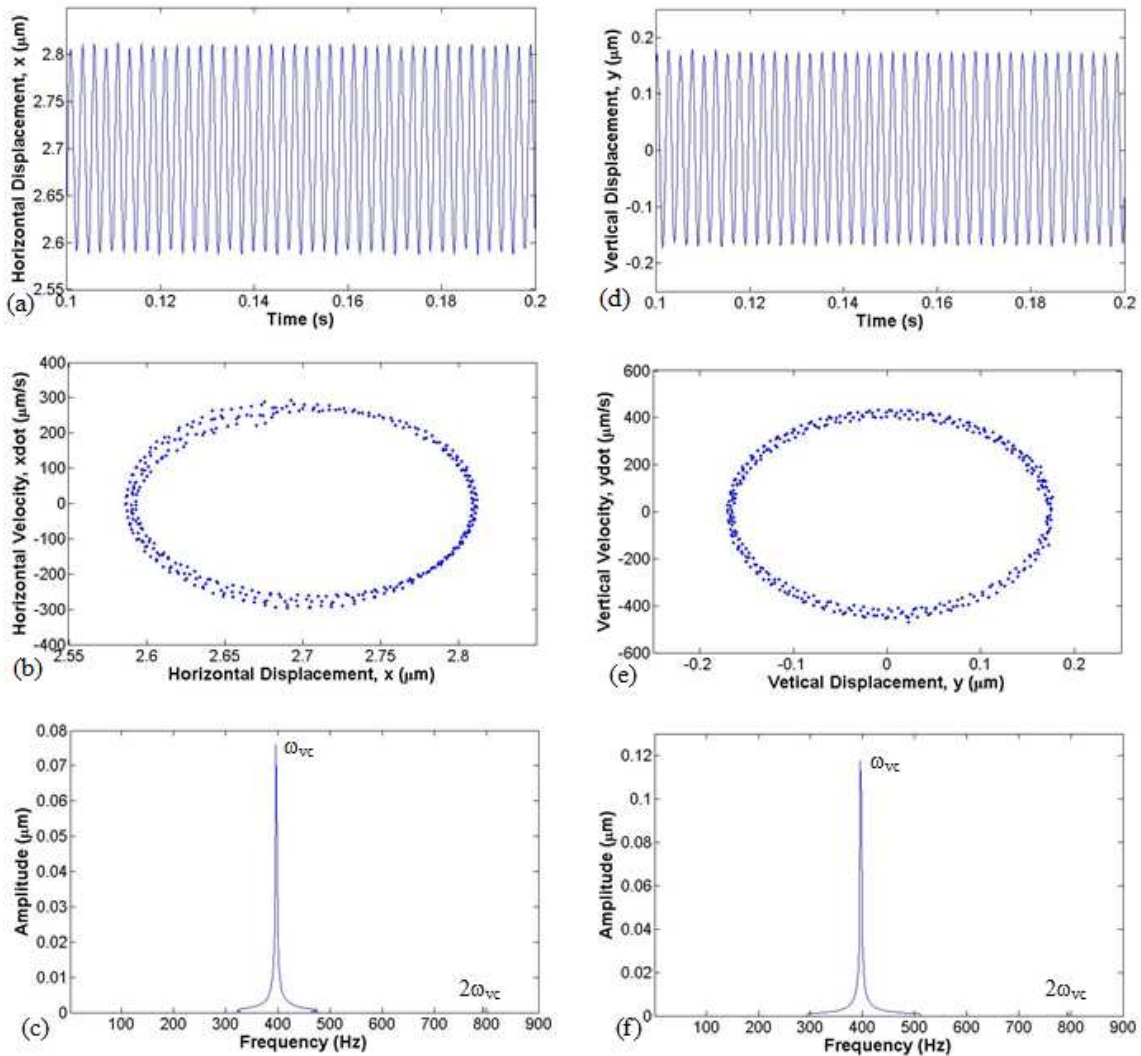


Figure 5. (a), (b), (c) Horizontal displacement response with time, Poincaré map for horizontal displacement response and FFT for horizontal displacement response at $N = 11$, respectively. (d), (e), (f) Vertical displacement response with time, Poincaré map for vertical displacement response and FFT for vertical displacement response at $N = 11$, respectively.

It is seen from the solutions of the effect of number of balls by certain conditions, the amplitude response are modulation. For few balls, the peak amplitudes of vibrations at the varying compliance frequency are more significant. The main reason for this is that increasing the number of balls means increasing the number of balls supporting the shaft therefore increasing the system stiffness and reducing the vibration amplitude in the vibration spectrum.

4. Conclusions

In this paper, a two degree of freedom nonlinear model of a rotor-ball bearing system has been developed to obtain the nonlinear vibration response by varying number of balls. Nonlinear analysis of this model was performed numerically using 4th order Runge-Kutta integration method. The results show that the characteristics of the dynamic behavior of the system are sensitive to small variation of the system parameters. Nonlinear response of an unbalanced rotor has been demonstrated to be chaotic with some specific combination of

number of balls and rotational speed of rotor. When the number of balls is increased, the center of oscillations approaches zero implying a stiffer system. So that increasing the number of balls will reduce the effect of the varying compliance frequency. Hence, the number of balls is an important parameter for vibration analysis of rotor bearing system and should be considered at the design stages of rotating machinery systems.

The identification of chaos, quasi-periodic oscillations, and route of chaos are very useful not only for efficient design of the rotor bearing systems but also useful in designing accurate diagnostic system for rolling element bearings. The model can therefore be used as a tool for predicting nonlinear dynamic behavior of rotor ball bearing system under different operating conditions. Moreover, the study may contribute to a further understanding of the nonlinear dynamics of rotor bearing system. Further, this detailed modeling is also very useful in development of accurate model for rolling elements bearings that will be helpful in improving the overall of rotating machineries. This is being pursued as future research.

Nomenclature

m	: Mass of rotor, kg
c	: Equivalent viscous damping factor, Ns/m
F_x	: Hertzian contact force on horizontal direction, N
F_y	: Hertzian contact force on vertical direction, N
F_u	: Force due to unbalance rotor, N
K	: Hertzian contact stiffness, $N/m^{3/2}$
N	: Number of balls
R_b	: Inner race radius, mm
R_a	: Outer race radius, mm
t	: Time, s
T	: Period, s
V_{cage}	: Translational velocity of the cage center, mm/s
V_a	: Translational velocity of the inner race, mm/s
V_b	: Translational velocity of the outer race, mm/s
W	: Radial load, N
γ	: Internal radial clearance, μm
ω_{rotor}	: Angular speed of rotor, rad/s
ω_{cage}	: Angular speed of the cage, rad/s
ω_a	: Angular speed of the inner race, rad/s
ω_b	: Angular speed of the outer race, rad/s
θ_j	: Angular location of j^{th} rolling element, rad/s

References

- [1] F. Ehrich, Observations of nonlinear phenomena in rotordynamics, *Journal of system design and dynamics* 2 (3), 641–651, 2008.
- [2] Mei Cheng, Guang Meng and Bingyu Wu, Nonlinear dynamics of a rotor-ball bearing system with Alford force, *Journal of Vibration and Control* 18(1), 17–27, 2011.
- [3] Dong-Soo Lee, Dong-Hoon Choi, A dynamic analysis of a flexible rotor in ball bearing with nonlinear stiffness characteristics, *International Journal of Rotating Machinery*, 3(2), 73-80, 1997.
- [4] El-Saeidy, F.M.A., Finite element modeling of rotor-shaft-rolling bearing system with consideration of bearing nonlinearities, *Journal of Vibration and Control* 4, 514-602, 1998.
- [5] Tiwari, M., Gupta, K., Prakash, O., Experimental study of a rotor supported by deep groove ball bearing, *International Journal of Rotating Machinery*. 8(4), 243-258, 2002.
- [6] Tiwari, M., Gupta, K., Prakash, O., Effect of radial internal clearance of a ball bearing on the dynamics of a balanced horizontal rotor, *Journal of Sound and Vibration*, 238(5, 723-756), 2000.
- [7] Wardle FP, Poon Y., Rolling bearing noise, cause and curve, *Chartered Mechanical Engineering*, 36-40, 1983.
- [8] Wardle FP., Vibration forces produced by waviness of the rolling surfaces of thrust loaded ball bearings. Part I: Theory *Proceeding of the IMechE*; 202(C5):305-12, 1988.
- [9] R. Zeillinger and H. Kötttritsch, Damping in a rolling bearing arrangement, *Evolution*, 1/96, 1996.
- [10] P. Lewis and S. B. Malanoski, Rotor-Bearing Dynamics Design Technology, Part IV: Ball Bearing Design Data. *AFAPL-TR-65-45*, 1965.
- [11] Krämer, E., *Dynamics of Rotor and Foundations*, Springer-Verlag, New York, 1993.
- [12] T.C. Gupta, K.Gupta, D.K. Sehgal, Nonlinear Dynamics and Chaos of an Unbalanced Flexible Rotor Supported by Deep Groove Ball Bearings with Radial Internal Clearance. *IUTAM Symposium on Emerging Trends in Rotor Dynamics*, 2011.
- [13] T.A. Harris, *Rolling Bearing Analysis*, 4th Edition, John Wiley & Sons, Inc., New York, 2001.
- [14] Francis C. Moon, Chaotic and Fractal Dynamics An Introduction for Applied Sciences and Engineers, *John Wiley & Sons, Inc.*, 1992.
- [15] Wenbing Tu, Yimin Shao, and Chris K. Mechefske, An analytical model to investigate skidding in rolling element bearings during acceleration, *Journal of Mechanical Science and Technology*, 26(8), 2451-2458, 2012.
- [16] Pyung Hwang, Van Trang Nguyen, A Study on Dynamic Analysis of Rotor-Bearing System with the Effect of Number of Balls, *Proceedings of KSTLE 56th - 2013 Spring Conference*, Seoul, Korea, 2013.

Biography



Van-Trang Nguyen received his B.S. in Mechanical Engineering from Vietnam National University, Ho Chi Minh City University of Technology in 2002 and M.S. degrees from Ho Chi Minh City University of Technical Education (HCM UTE) in 2004 respectively. He then received his Ph.D degree from Yeungnam University, Korea.

He is currently a lecturer at the Ho Chi Minh City University of Technology and Education, Vietnam. His research interests focus on rotordynamics, internal combustion engine, electric vehicle, and mechanical vibration.

E-mail address: trangnv@hcmute.edu.vn



Pyung Hwang received his B.S. in Mechanical Design & Production Engineering, M.S., and Ph.D. degrees from Seoul National University in 1979, 1981 and 1989 respectively. He is now a Professor of the School of Mechanical Engineering, Yeungnam University, Korea. His current research interests include Tribology, and

Rotordynamics